International Journal of Informatics and Communication Technology (IJ-ICT)
Vol. 14, No. 3, December 2025, pp. 993~1001
ISSN: 2252-8776, DOI: 10.11591/ijict.v14i3.pp993-1001

Design of miniaturized dual-band bandpass filter with enhanced selectivity for GPS and RFID applications

Thupalli Shaik Mahammed Basha[1], Arun Raaza[2], Vishakha Bhujbal[3], Meena Mathivanan[4]
[1]Department of Electronics and Communication Engineering, Vels Institute of Science, Technology and Advanced Studies, Chennai, India
[2]Vels Institute of Science, Technology and Advanced Studies, Chennai, India
[3]MET Institute of Management, Mumbai, India
[4]Department of Electronics and Communication Engineering, Vels Institute of Science, Technology and Advanced Studies, Chennai, India

Article Info

Article history:

Received Aug 20, 2024
Revised Dec 14, 2024
Accepted Jan 19, 2025

Keywords:

Bandpassfilter
Dual-band
High selectivity
Interdigital coupled line
Miniaturization
Transmission zeros

ABSTRACT

This article presents a miniaturized interdigital coupled dual-band bandpass filter with multiple transmission zeros/poles. Stepped impedance resonators, interdigital coupled lines, and series coupled lines make up the proposed filter design. A circuit simulator is used to analyze a proposed filter, and the magnitude and bandwidth shifts have been investigated. To confirm the proposed filter design, equations for transmission zero frequencies have been constructed and verified based on even-odd mode analysis and lossless transmission line theory. A working prototype for 2.2 GHz (RFID) and 1.38 GHz (GPS) applications is made and tested. With λg representing the guided wavelength at the first band (1.38GHz), the finished prototype is compact, measuring 0.32 λg×0.27 λg. According to the experimental findings, there is strong selectivity in the first and second passbands, with roll-off rates of 190 and 168 dB/GHz, respectively. Good isolation between the two passbands is indicated by an insertion loss of less than 20 dB.

Corresponding Author:

Thupalli Shaik Mahammed Basha
Department of Electronics and Communication Engineering
Vels Institute of Science, Technology and Advanced Studies (VISTAS)
Chennai, India
Email: mahammadbasha.ece@jntua.ac.in

1. INTRODUCTION

In the realm of modern wireless communication systems, the demand for efficient and versatile bandpass filters has surged, driven by the need for enhanced signal quality and spectrum utilization. Among the various filter designs, dual-band microstrip bandpass filters have garnered significant attention due to their compact size, ease of integration, and ability to operate across multiple frequency bands simultaneously. By leveraging advanced electromagnetic modeling techniques and innovative substrate materials, these filters offer superior performance characteristics such as improved bandwidth, higher selectivity, and lower insertion loss. Such attributes are crucial for enhancing the efficiency and reliability of communication systems in applications ranging from satellite communications and radar systems to wireless sensor networks and medical telemetry.

The literature introduces the design of a microstrip dual-band bandpass filter with closely specified passbands [1]-[4]. Precise control over the passband frequencies and bandwidths is achieved through meticulous design and optimization of the microstrip layout. A high selectivity compact dual-band bandpass filter with seven transmission-zeros designed for GPS and WiMAX applications is discussed in the literature [5], [6].

The use of multiple transmission-zeros enhances the filter's selectivity and out-of-band rejection, ensuring high performance in demanding environments. This design approach provides a robust solution for dual-band operation in critical communication applications. Research investigates both single- and dual-band bandpass filters employing coupled stepped-impedance resonators with embedded coupled-lines [7]. This approach achieves enhanced coupling and improved filter performance. An article presents a dual-band high-temperature superconducting hairpin-resonator bandpass filter that operates based on two pairs of nondegenerate modes [8]. The use of high-temperature super conducting materials significantly reduces losses, resulting in higher quality factors and better filter performance. The design of dual-band interdigital bandpass filters utilizing both series and shunt resonators was studied [9], [10]. The combination of these resonators enables the creation of filters with precise control over the passbands and transmission zeros, resulting in high-performance filters with improved out-of-band rejection.

A study introduces a high-selectivity tunable dual-band bandpass filter using stub-loaded stepped-impedance resonators [11]. This configuration provides flexibility in achieving narrowband and wideband responses, making it ideal for various wireless communication applications. The design of an on-chip dual-band bandpass filter using lumped elements in low-temperature co-fired ceramic (LTCC) technology was studied [12], [13]. The integration of lumped elements on-chip allows for miniaturization and compatibility with monolithic microwave integrated circuits (MMICs). A compact lowpass and dual-band bandpass filter with controllable transmission zeros, center frequencies, and passband bandwidth was analyzed [14]. The compact size and controllable characteristics make this filter an attractive option for multifunctional communication systems. The use of varactor diodes allows for real-time tuning of the filter's center frequencies, making it adaptable to varying operational requirements [15]. The literature introduces a dual-band balanced bandpass filter utilizing slot lines loaded patch resonators, enabling independent control of bandwidths for each passband [16]. The innovative design allows for precise adjustments of resonant frequencies and bandwidths, providing high flexibility in filter applications.

A dual-band balanced bandpass filter developed using electrically small planar resonators features excellent common-mode suppression, critical for maintaining signal integrity in differential signaling environments [17]. The compact size of the resonators and efficient suppression of common-mode noise make this filter suitable for high-density electronic circuits and systems. The design of dual-band bandpass filters based on metal-integrated suspended line technology is studied in this article [18]. The use of suspended lines offers low insertion loss and high-quality factors, enhancing overall filter performance. This work presents a bandpass filter that can be tuned across a wide frequency range while maintaining high selectivity [19]. The proposed design focuses on improving frequency selectivity and achieving a wide tuning range, which is significant for applications requiring versatile frequency management. It utilizes frequency-dependent S-L (series-to-line) coupling to achieve high selectivity and compact size, making it suitable for applications with stringent size and performance requirements [20].

This article describes a tunable bandpass filter covering a frequency range from 0.86 to 3.83 GHz [21]. The filter is designed to offer high selectivity across its entire tuning range, which is beneficial for radio frequency (RF) and microwave applications requiring precise frequency filtering. The paper presents a dual-band bandpass filter with constant absolute bandwidth and reconfigurable bandwidth capability [22]-[24]. The filter utilizes a mode control technique to adjust bandwidth, making it versatile for applications needing adjustable dual-band operation. This research introduces a bandpass filter that can intrinsically switch between constant absolute bandwidth (CABW) and constant fractional bandwidth (CFBW) modes [25] The filter's design allows for flexible bandwidth management and is suitable for diverse electronic applications requiring adaptable filtering characteristics. In the recently reported literature has low selectivity in passband to stop band or stop band to stop band. Therefore, in this proposed work address all these issues.

This brief proposes a miniaturized second order interdigital line loaded dual band pass filter which generates two transmission poles in each passband and five transmission zeros in the stopband. The prosed filter has enhanced skit rate due to the presence of multiple transmission zeros/poles. In the presented filter consists of two set of interdigital coupled lines and meandering open stubs and two feeding ports. The fabricated and experimentally validated filter layout is etched on Rogers RT/Duriod 5880 substrate. The fabricated filter’s filtering characteristics are matched with the simulated and theoretical response.

2. RESEARCH METHOD

Figures 1 and 2, Figures 1(a) and (b) show the proposed dual band bandpass filter's layout and transmission line design, respectively. A shunt-coupled line ($1/Y_{E1}$, $1/Y_{O1}$,θ), loaded with a pair of open stubs ($1/Y_3$,θ), two series-coupled lines ($1/Y_{E2}$, $1/Y_{O2}$,θ), and stepped-impedance open-stubs ($1/Y_1$,θ) and ($1/Y_2$,θ)make up this arrangement. An Ansys HFSS 2024R1 is used to simulate the suggested filter setup, and the equivalent circuit is presented in Figure 1(c). Two passbands, with a return loss of more than 22 dB in each, are present in the circuit-simulated response, which is centered at 1.38 and 2.2 GHz. In addition, this filter has five transmission zeros (TZs) in the stopband and two transmission poles (TPs) in each passband. The presented filter setup is investigated using a lossless transmission line model method. The designed filter's optimized physical dimensions are tabulated in Table 1.

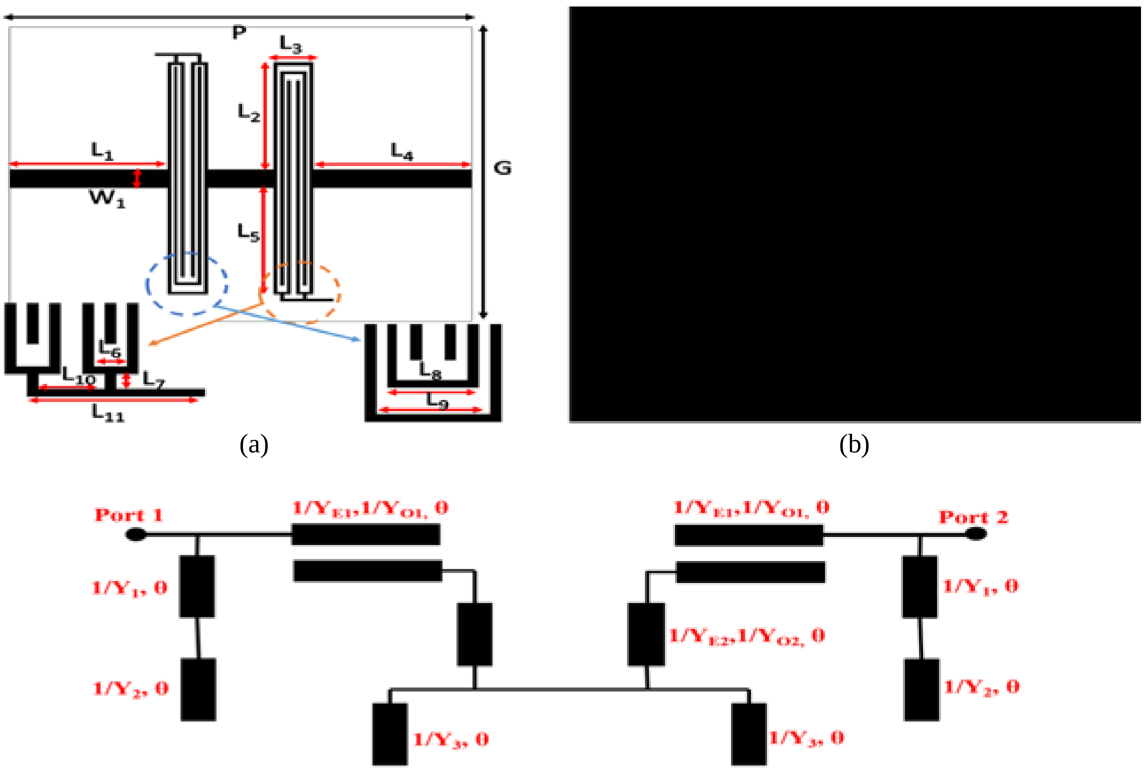

Figure 1. The dual band bandpass filter: (a) structure top view, (b) bottom view, and (c) equivalent circuit analysis

Table 1. The presented dual-band pass filter physical dimension

Parameter	Value (Mm)	Parameter	Value (Mm)	Parameter	Value (Mm)	Parameter	Value (Mm)	Parameter	Value (Mm)
P	33	L_2	13	L_5	12	L_8	1.75	L_{11}	7
G	35	L_3	3	L_6	1.25	L_9	3.25	W_1	2
L_1	12	L_4	10	L_7	0.75	L_{10}	2		

A band stop response with three TZs (fTZ3, fTZ4, and fTZ5) is produced by the cascaded section of shunt coupled line and parallel open stubs when the impedance values are appropriately chosen [21]. A wide passband response is offered by the open circuited stub transmission lines. The combination of the band stop section and series linked lines truncates this wide passband response into two narrow passbands. Furthermore, TZs (fTZ2, fTZ6) are inserted in the lower and higher stop bands by using stepped impedance open-stubs in order to increase the selectivity on the lower and upper sides of the passband. Researcher [17]-[21], the selectivity is not enhanced in both the stop band to pass band and pass band to stop band. 1/Y1 and 1/Y2 impedances controls the TZ positions [22]. Even-odd mode analysis is used to validate the filter's TZ frequencies while the proposed filter construction is symmetric. The even and odd transmission line models are shown in Figures 2(a) and 2(b), respectively. These are the even and odd mode input impedances that are determined using the loss free transmission line theory [23]. The total admittance variation of the filter is derived with the help of equivalent circuit model and it is given in (1) to (12).

$$\frac{1}{y_{inE}} = \frac{\frac{1}{Y_{SIS}Y_{CE}}}{\frac{1}{Y_{SIS}}+\frac{1}{Y_{CE}}} \tag{1}$$

$$\frac{1}{y_{inO}} = \frac{\frac{1}{Y_{SIS}Y_{CO}}}{\frac{1}{Y_{SIS}}+\frac{1}{Y_{CO}}} \quad (2)$$

Where,

$$\frac{1}{Y_{CE}} = -jA_{C1}\cot\theta + \frac{\frac{1}{Y_{C2}^{2}}csc^{2}\theta}{\frac{1}{Y_{PE}+\frac{1}{jY_{C1}}\cot\theta}} \quad (3)$$

$$\frac{1}{Y_{CO}} = -jA_{C1}\cot\theta + \frac{\frac{1}{Y_{C2}^{2}}csc^{2}\theta}{\frac{1}{Y_{PO}+\frac{1}{jY_{C1}}\cot\theta}} \quad (4)$$

$$\frac{1}{Y_{C1}} = \frac{\frac{1}{Y_{E1}}+\frac{1}{Y_{O1}}}{2} \quad (5a)$$

$$\frac{1}{Y_{C2}} = \frac{\frac{1}{Y_{E1}}-\frac{1}{Y_{O1}}}{2} \quad (5b)$$

$$\frac{1}{Y_{PE}} = \frac{1}{Y_{E2}}\left[\frac{\frac{1}{Y_{OC1}}-\frac{1}{jY_{E2}\tan\theta}}{\frac{1}{Y_{E2}}-\frac{1}{jY_{OC2}\tan\theta}}\right] \quad (5c)$$

$$\frac{1}{Y_{OC1}} = \frac{1}{-jY_{3}\cot\theta} \quad (6)$$

$$\frac{1}{Y_{PO}} = \frac{1}{-jY_{O2}\tan\theta} \quad (7)$$

$$\frac{1}{Y_{AIS}} = \frac{1}{JY_{1}}\left[\frac{\frac{1}{Y_{1}}\tan\theta-\frac{1}{Y_{2}\cot\theta}}{\frac{1}{Y_{1}}+\frac{1}{Y_{2}}}\right] \quad (8)$$

It is possible to define the S-parameters of the recommended dual bandpass filter in terms of even and odd mode admittances as,

$$S_{11} = \frac{\left(\frac{1}{Z_{0}}\right)^{2}-\left(\frac{1}{Z_{inE}Z_{inO}}\right)}{\left(\frac{1}{z_{0}}+\frac{1}{Z_{inE}}\right)\left(\frac{1}{z_{0}}+\frac{1}{Z_{inO}}\right)} \quad (9a)$$

$$S_{11} = \frac{\frac{1}{Z_{O}}\left(\frac{1}{Z_{inE}}\right)-\left(\frac{1}{Z_{inO}}\right)}{\left(\frac{1}{z_{0}}+\frac{1}{Z_{inE}}\right)\left(\frac{1}{z_{0}}+\frac{1}{Z_{inO}}\right)} \quad (9b)$$

by setting S_{21}=0, the circuit-simulated TZ frequencies of the suggested filter may be confirmed, yielding,

$$\frac{1}{Y_{sis}}\left(\frac{1}{Y_{CE}}-\frac{1}{Y_{CO}}\right) = 0 \quad (10a)$$

$$\frac{1}{Y_{sis}} = 0 \text{ and } \frac{1}{Y_{CE}}-\frac{1}{Y_{CO}} = 0$$

simplifying $\frac{1}{Y_{sis}} = 0$, we get,

$$\theta = \theta_{TZ2} = \cot^{-1}\left(\sqrt{\frac{Y_{2}}{Y_{1}}}\right) \quad (10b)$$

simplifying $\frac{1}{Y_{CE}} = \frac{1}{Y_{CO}}$, we get,

$$tan^2\theta\left(\frac{1}{Y_{E2}Y_{O2}}+\frac{1}{Y_3Y_{O2}}-\left(\frac{1}{Y_{E2}}\right)^2\right)=\frac{-1}{Y_{E2}Y_3} \quad (11a)$$

$$\theta=\theta_{TZ3}=tan^{-1}\left(\sqrt{\frac{\frac{-1}{Y_{E2}Y_3}}{\frac{1}{Y_{E2}Y_{O2}}+\frac{1}{Y_3Y_{O2}}-\left(\frac{-1}{Y_{E2}}\right)^2}}\right) \quad (11b)$$

The TZ frequencies may be found using (9) based on the link between electrical length and design frequency.

$$f_{TZn}=\frac{\theta_{TZn}}{\theta_0}f_0(n=2,3,5,6) \quad (12)$$

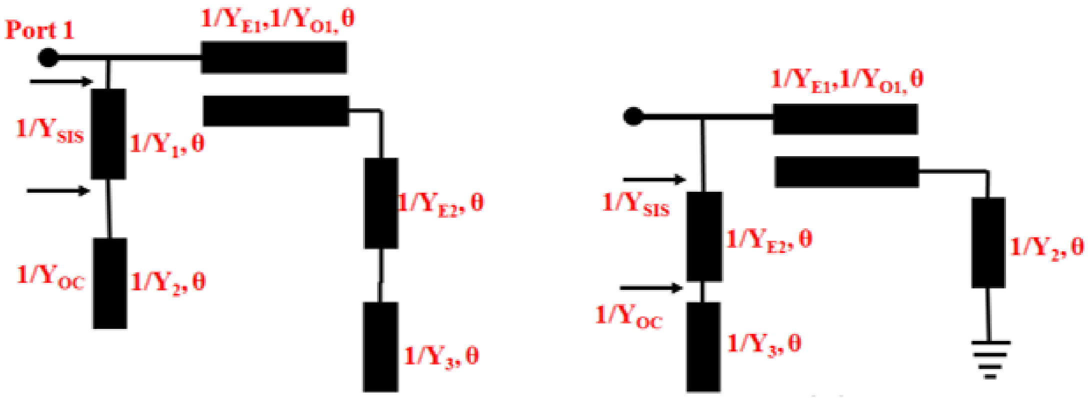

Figure 2. The presented dual band pass filter equivalent circuit (a) even mode and (b) odd mode

The series connected lines' intrinsic zeros are the TZs at f_{TZ1}=0 and f_{TZ7}=2f_0 [18]. The f_{TZ2} and f_{TZ3} may be derived from (7)–(10). Since the response is symmetric, 2f_0- f_{TZ3} and 2f0- f_{TZ2}, respectively, can provide f_{TZ5} and f_{TZ6}. In (7), the denominator and numerator reach infinity at the same time when θ=90◦ (f_0=1 GHz). But the higher-order denominator gets closer to infinity first, creating a TZ at f_{TZ4}. The computed seven TZ frequencies are 0.5, 0.91, 1.89, 2.05, and 2.59 GHz, and they are perfectly complement with the circuit simulated ones proving the proposed filter structure. Having into consideration $1/Y_{E1}$=190, $1/Y_{O1}$=85, $1/Y_{E2}$=132, $1/Y_{O2}$=77, $1/Y_1$=130, $1/Y_2$=78, $1/Y_3$=110, θ=90, and f_0=1 GHz.

Varying the impedances ($1/Y_1$, $1/Y_2$, $1/Y_3$) and coupling coefficients (K_1=($1/Y_{E1}$–$1/Y_{O1}$)/($1/Y_{E1}$+$1/Y_{O1}$) and K2=($1/Y_{E2}$-$1/Y_{O2}$)/($1/Y_{E2}$+$1/Y_{O2}$) of the proposed dual band bandpass filter allows to study the magnitude response of the circuit simulation. The return loss in both passbands increases when $1/Y_1$ and $1/Y_2$ decreases. $1/Y_3$ enhances the passbands' return loss and improves the inter-stopband's rejection level. As K_1 increases, so does the distance between the pass bands. An increase in K_2 improves the inter-stopband responsiveness. This research suggests that by appropriately choosing the impedances of the proposed structure, it is possible to regulate the centre frequencies of two passbands with good matching. The change of the pass bands' 3 dB FBWs for various values of the presented dual band bandpass filter is shown in Figure 3. There is less variability in the 3-dB FBWs as $1/Y_1$ and $1/Y_2$increases. While it lowers as K_2 grows, the 3 dB FBWs of both passbands increase when $1/Y_3$ and K_1 increase as shown in Figures 3(a) to 3(e).

3. RESULTS AND DISCUSSION

In this section, it is explained the results of research and at the same time is given the comprehensive discussion. Section 2 analysis and the design process described in [24] led to the finalized values of $1/Y_{E1}$=190, $1/Y_{O1}$=75, $1/Y_{E2}$=121, $1/Y_{O2}$=55, $1/Y_1$=140, $1/Y_2$=92, $1/Y_3$=120, θ=90°, and f_0=2.4 GHz for the circuit implementation. The develop and simulate the proposed dual band bandpass filter using Ansys HFSS V 2014R1 full-wave EM simulator. For the construction of the presented filter, Rogers RT/Duriod 5880 substrate with a dielectric constant of 2.2, a thickness of 0.78 mm, and a loss tangent of 0.0009 is employed. The comparison of simulated and measured S-parameter responses and fabricated pictures are plotted in Figure 4. From Figure 4, both the bands return loss are enhanced compared with the all other dual band pass filter responses.

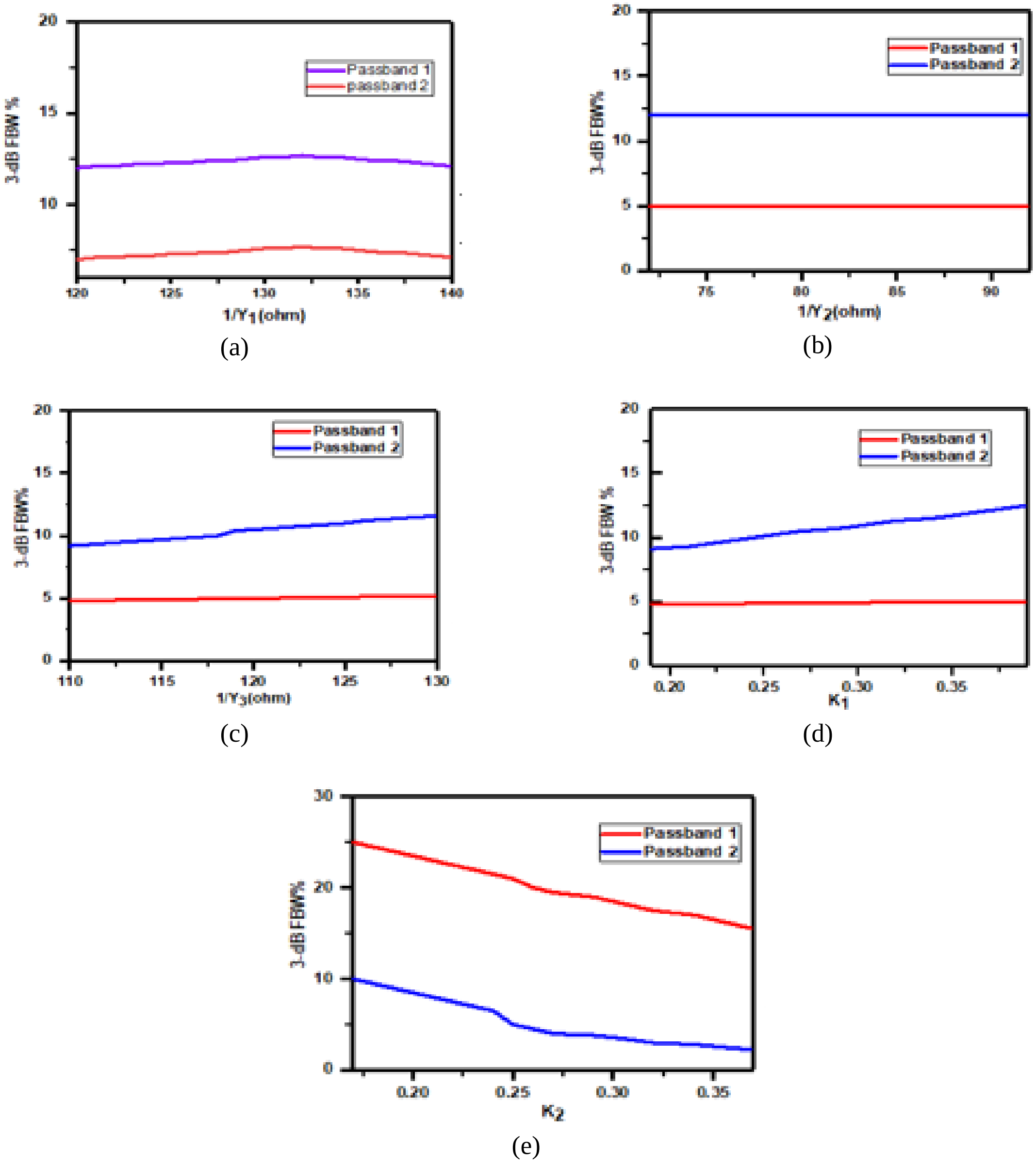

Figure 3. Lower and upper band filter's 3 dB-FBW variation: (a) $1/Y_1$, (b) $1/Y_2$, (c) $1/Y_3$, (d) K_1, and (e) K_2

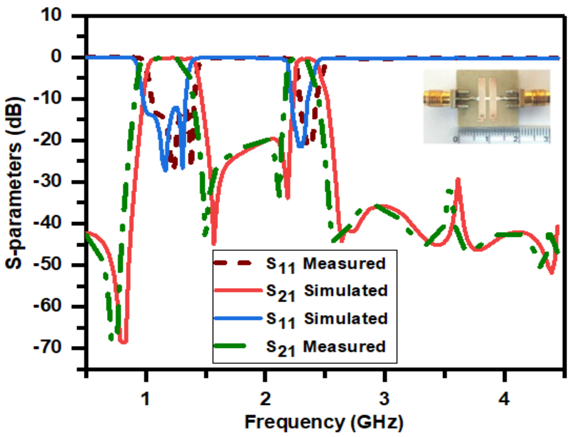

Figure 4. Simulated and measured S-parameter response

A vector network analyzer is used to assess the group latency and magnitude responses of the proposed dual band bandpass filter. The two passbands with frequencies centred at 1.35 GHz and 2.2 GHz had their tested 3 dB FBWs determined to be 14.33% and 6.59%, respectively. At 1.35 and 2.2 GHz, the observed insertion losses are 1.2 dB and 1.1 dB, respectively. In the first passband, the measured return losses are 21 dB, and in the second passband, they are 19.8 dB. The simulated and measured group delay is illustrated in Figure 5.

The first band's tested roll-off rate is 190 dB/GHz, while the second band's is 168 dB/GHz. These results are more precise than the ones found in [2], [7], [9], [11], [12], [15], [17]. Figure 5(b) shows the measured group delay of the presented dual band bandpass filter. Group delay ranges from 2.1 to 5.2 ns in the first passband and from 2.4 to 6.6 ns in the second. The simulated and measured values varied somewhat because of measurement uncertainties and manufacturing tolerances. The simulated and measured group delay is illustrated in Figures 5(a) and 5(b).

Table 2 presents a comparison of the proposed dual band bandpass fitler's performance with previous reported efforts. With similar 3 dB FBWs and more transmission zeros, the recommended filter is less in size. It is possible to scale the design for various dual-band applications because it is built on a transmission line concept.

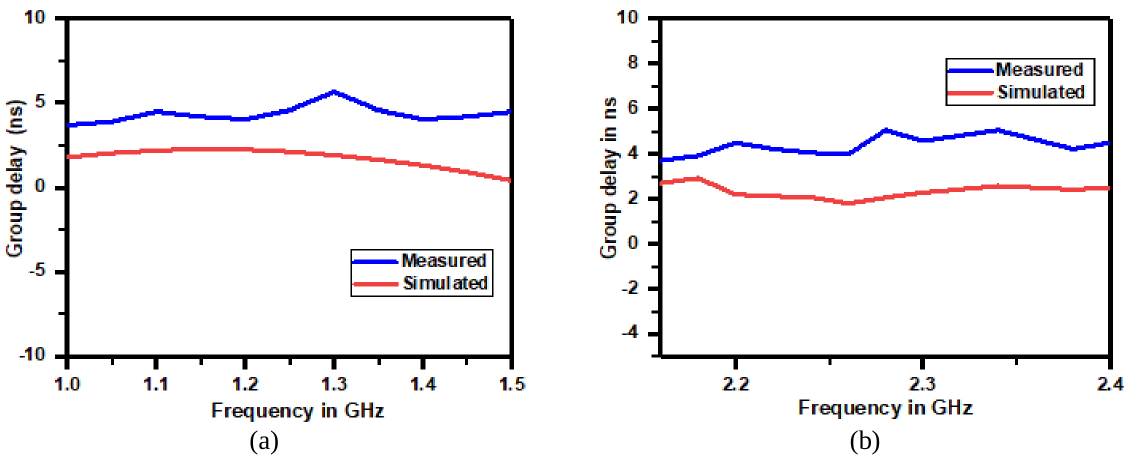

Figure 5. Simulated and measured group delay response (a) lower band and (b) upper band

Table 2. Proposed dual-band bandpass filters performance comparison with other reported filters

Reference	f_1, f_2	f_1/f_2	3-dB FBW (%)	No. of TZs	Order (N)	Size ($\lambda_g \times \lambda_g$)	Applications
[2]	2.1, 5.9	2.12	7.0/4.0	3	1	0.27×0.27	GSM, ISM
[7]	2.45, 5.45	3.22	2.4/2.3	2	2	0.33×0.42	ISM, Wi-Max
[9]	2.45, 4.3	1.50	2.22/1.70	3	3	0.72×0.34	ISM, Wi-Fi
[11]	1.9, 3.15	2.25	7.0/5.5	1	2	0.66×0.54	ISM
[12]	2.4, 5.2	2.08	10.7/5.4	4	2	0.92×0.59	-
[15]	2.2, 3.9	3.8	6.5/4.9	5	3	0.88×0.72	-
[17]	2.45, 5.1	1.49	3.3/4.6	2	2	0.58×0.67	ISM, WLAN
This work	1.35, 2.2	2.1	2.9/2.6	4	2	0.32×0.27	GPS, Wi-Max

4. CONCLUSION

Using two stepped impedance resonators, meandering open stubs and interdigital coupled line, a minimized dual-band bandpass filter is proposed and realized. Seven transmission zeros are included in the stopband of the presented filter, and its passband response is second-order. The presented filter's lower band operates at 1.34 GHz for GPS and the upper band operates at 2.2 GHz for RFID applications. Better isolation between the passbands, selectivity, and fractional bandwidth are all features of the designed filter.

FUNDING INFORMATION

This work is not funded by any funding agencies.

AUTHOR CONTRIBUTIONS STATEMENT

Name of Author	C	M	So	Va	Fo	I	R	D	O	E	Vi	Su	P	Fu
Thupalli Shaik	✓	✓	✓	✓	✓	✓		✓	✓	✓			✓	
Mahammed Basha														
Arun Raaza		✓				✓		✓	✓	✓	✓	✓		
Vishakha Bhujbal	✓		✓	✓			✓			✓	✓	✓	✓	
Meena Mathivanan		✓				✓	✓	✓			✓		✓	

C : **C**onceptualization
M : **M**ethodology
So : **So**ftware
Va : **Va**lidation
Fo : **Fo**rmal analysis
I : **I**nvestigation
R : **R**esources
D : **D**ata Curation
O : Writing - **O**riginal Draft
E : Writing - Review & **E**diting
Vi : **Vi**sualization
Su : **Su**pervision
P : **P**roject administration
Fu : **Fu**nding acquisition

CONFLICT OF INTEREST STATEMENT

Authors state no conflict of interest.

DATA AVAILABILITY

No data was used for the research described in the article.

REFERENCES

[1] Q. Zhang, H. Liu, and X. Sun, "Microstrip dual-band bandpass filter design with closely specified passbands," *IEEE Microwave and Wireless Components Letters*, vol. 22, no. 2, pp. 56–58, Feb. 2012.

[2] Y. Li, W. Chu, and T. X. Cao, "Design of high selectivity compact dual-band bandpass filter with seven transmission-zeros for GPS and WiMAX applications," *IEEE Transactions on Microwave Theory and Techniques*, vol. 61, no. 3, pp. 1316–1324, 2013.

[3] L. Gao, X. Y. Zhang, and Q. Xue, "Single- and dual-band bandpass filters using coupled stepped-impedance resonators with embedded coupled-lines," *IEEE Transactions on Microwave Theory and Techniques*, vol. 61, no. 9, pp. 3183–3193, Sep. 2013.

[4] Y. He, H. Tian, and X. Liu, "Dual-band high-temperature superconducting hairpin-resonator bandpass filter based on two pairs of nondegenerate modes," *IEEE Transactions on Applied Superconductivity*, vol. 24, no. 5, pp. 1–5, Oct. 2014.

[5] X. Chen, K. Song, and Y. Fan, "Design of dual-band interdigital bandpass filters using both series and shunt resonators," *IEEE Transactions on Microwave Theory and Techniques*, vol. 62, no. 2, pp. 337–345, Feb. 2014.

[6] J. Wang, Z. Ma, and H. Liu, "A high-selectivity tunable dual-band bandpass filter using stub-loaded stepped-impedance resonators," *IEEE Microwave and Wireless Components Letters*, vol. 25, no. 2, pp. 91–93, Feb. 2015.

[7] S. Sun, M. F. Lei, and R. Xu, "Design of on-chip dual-band bandpass filter using lumped elements in LTCC technology," *IEEE Transactions on Components, Packaging and Manufacturing Technology*, vol. 5, no. 9, pp. 1318–1326, Sep. 2015.

[8] C. Zhu, L. Zhu, and H. Zhang, "Compact lowpass and dual-band bandpass filter with controllable transmission zero/center frequencies/passband bandwidth," *IEEE Transactions on Microwave Theory and Techniques*, vol. 63, no. 3, pp. 1080–1090, 2015.

[9] J. Xu, W. Wu, and C. Miao, "Varactor tuned dual-band bandpass filter with independently tunable band positions," *IEEE Transactions on Circuits and Systems II: Express Briefs*, vol. 62, no. 4, pp. 321–325, Apr. 2015.

[10] X. Xiong, B. Z. Wang, and Y. X. Wang, "Dual-band balanced bandpass filter using slotlines loaded patch resonators with independently controllable bandwidths," *IEEE Transactions on Microwave Theory and Techniques*, vol. 67, no. 1, pp. 89–98, 2019.

[11] H. Wang, W. Kang, and Y. Li, "Dual-band balanced bandpass filter with common-mode suppression based on electrically small planar resonators," *IEEE Microwave and Wireless Components Letters*, vol. 27, no. 6, pp. 523–525, Jun. 2017.

[12] Z. Huang, S. Zhang, and Q. Xue, "Design of dual-band bandpass filters based on metal-integrated suspended line technology," *IEEE Transactions on Microwave Theory and Techniques*, vol. 64, no. 3, pp. 689–696, Mar. 2016.

[13] K. Song, X. Wang, C. Zhong, Y. Chen, and Y. Fan, "Wide-frequency tunable bandpass filter with high-frequency selectivity," *Electromagnetics*, vol. 39, no. 6, pp. 430–442, 2019, doi: 10.1080/02726343.2019.1677121.

[14] Y. Zhu, L. Xue, F. Sun, F. Liu, and H. Deng, "Compact high-selectivity tunable dual-mode filter with constant bandwidth by adopting frequency-dependent S-L coupling," *Microwave and Optical Technology Letters*, vol. 62, no. 1, 2019, doi: 10.1002/mop.32117.

[15] X. Wang, D. Zhang, Q. Liu, D. Lv, Y. Zhang, and S. Yang, "A tunable 0.86–3.83 GHz bandpass filter with high selectivity," *International Journal of RF and Microwave Computer-Aided Engineering*, vol. 30, no. 4, 2020, doi: 10.1002/mmce.22055.

[16] S. Narayana, N. Kumar, and Y.-K. Singh, "Constant absolute bandwidth tunable asymmetric order dual-band BPF with reconfigurable bandwidth using mode control technique," *IET Microwaves, Antennas and Propagation*, vol. 15, no. 3, pp. 253–270, 2021, doi: 10.1049/mia2.12134.

[17] T.-J. Du, B.-R. Guan, P.-Q. Zhang, Y. Gu, and D.-J. Wei, "An intrinsically switched tunable CABW/CFBW bandpass filter," *Electronics*, vol. 10, no. 11, 2021, doi: 10.3390/electronics10111234.

[18] B. Mushtaq and S. Khalid, "Design of miniaturized single and dual-band bandpass filters using diamond-shaped coupled line resonator for next-generation wireless systems," *International Journal of Microwave and Wireless Technologies*, vol. 15, no. 3, pp. 375–383, 2023, doi: 10.1017/S1759078722001416.

[19] B. Mushtaq, M. A. Rehman, A. Hussain, and M. J. Abbass, "A highly selective dual bandpass filter using coupled line resonator for modern wireless communication systems," in *Proceedings of the 2023 4th International Conference on Computing, Mathematics and Engineering Technologies (iCoMET)*, Sukkur, Pakistan, 2023, pp. 1–5, doi: 10.1109/iCoMET57998.2023.10099212.

[20] G. Pachaiyappan and P. Ramanujam, "Design of low profile co-axial fed high gain stacked patch antenna for Wi-Fi/WLAN/WiMAX applications," *Frequenz - Journal of RF-Engineering and Telecommunications*, vol. 75, no. 1–2, pp. 27–34, 2021.

[21] P. Ramanujam, K. Ramanujam, and M. Ponusamy, "A novel asymmetrical interdigital coupled line-based penta-band bandpass filter design with enhanced selectivity employing square complementary split ring resonator," *International Journal of RF and Microwave Computer-Aided Engineering*, e22888, Aug. 2021.
[22] P. Sambathkumar, K. Ramanujam, and P. Ramanujam, "Design of 6×2 linear feed antenna array with suppressed SLL by employing CCSRR for Ka-band and 5G mm-wave applications," *Applied Physics A*, vol. 129, no. 4, p. 287, 2023.
[23] X.-B. Zhao, F. Wei, P. F. Zhang, and X. W. Shi, "Mixed-mode Magic-Ts and their applications on the designs of dual-band balanced out-of-phase filtering power dividers," *IEEE Transactions on Microwave Theory and Techniques*, vol. 71, no. 9, pp. 3896–3905, Sep. 2023.
[24] V. K. Killamsetty and B. Mukherjee, "Compact dual bandpass filter for terrestrial radio and GSM applications," *International Journal of RF and Microwave Computer-Aided Engineering*, vol. 27, no. 8, p. 21131, 2017.
[25] Y. Wu, Q. Zeng, and Y. Shang, "A low-insert loss and high-return loss bandpass filter based on cut-off rectangular waveguide for satellite communication application," *International Journal of RF and Microwave Computer-Aided Engineering*, vol. 31, no. 2, p. 22351, 2021.

BIOGRAPHIES OF AUTHORS

Mr. Thupalli Shaik Mahammed Basha is working as an assistant professor in the electronics and communication engineering at JNTU Institute of Engineering, Pulivendula and Research Scholar of Vels Institute of Science, Technology and Advanced Studies, Chennai. He graduated in engineering at Madina College of Engineering, India. He secured master of engineering in digital electronics and communication system at AITS College of Engineering, Rajampet, India. He Pursuing Ph.D. in electronics and communication engineering at Vels Institute of Science, Technology and Advanced Studies, Chennai, Tamil Naadu, India. He is in the field of antenna design of dual band pass filter for MMW applications at Vels Institute of Science, Technology and Advanced Studies, Chennai, Tamil Nadu, India. He is in teaching profession for more than 12 years. He has presented 25 papers in national and international journals, conference and symposiums. His main area of interest includes antenna design, wireless communication, wireless networks. He is a life Member of Indian Society for Technical Education (ISTE) (LM90075). He can be contacted at email: mahammadbasha.ece@jntua.ac.in.

Dr. Arun Raaza is an accomplished researcher and innovator affiliated with Vels Institute of Science, Technology and Advanced Studies (VISTAS) as Director of Centre for Advanced Research and Development. He holds a Ph.D. degree in electronics and communication engineering and has a rich academic journey spanning in prestigious institutions across India and Swansea University, United Kingdom. Dr.Raaza's extensive research portfolios includes 110+ national patents, 6+ international patents, 50+ peer reviewed publications, 4+books published and contributions to several funded or sponsored research projects in collaboration with various government and industry entities. His commitment to fostering innovation and setting up innovation labs globally, resulting in numerous accolades and awards for both himself and his mentees. He is also Founder CEO of ARCOMM a leading technical child skill development company having its presence in India, UAE and Oman and Co-Founder/Director of STRICX LLC, USA. He can be contacted at email: director.card@velsuniv.ac.in.

Mrs. Vishakha Bhujbal is the senior management representative of Mumbai Educational Trust, Bhujbal Knowledge City. She graduated from Pune University, pursuing psychology and sociology while majoring in Sanskrit. She completed her post-graduation from Mumbai University and holds an MBA in human resources to understand better the emerging challenges critical for shaping professionals. Presently, she is pursuing her doctorate. A young and dynamic educational and social activist, she works tirelessly in the challenging area of shaping youth, from tiny tots to young professionals, preparing them to play meaningful roles in building an inclusive society. She can be contacted at email: vishakhap1911@gmail.com.

Dr. Meena Mathivanan is working as an associate professor in the electronics and communication engineering at Vels Institute of Science, Technology and Advanced Studies, Chennai. She graduated in engineering at Sardar Raja College of Engineering, Tirunelveli, Tamil Nadu, India. She secured Master of Engineering in Applied Electronics at Jerusalem college of Engineering, Chennai, Tamil Nadu, India. She secured Ph.D., in wireless networks at Vels Institute of Science, Technology and Advanced Studies, Chennai, Tamil Naadu, India. She is in the field of cognitive radio network at Vels Institute of Science, Technology and Advanced Studies, Chennai, Tamil Nadu, India. She can be contacted at email: meena.se@velsuniv.ac.in.